Computational Analysis of Williamson Fluid Flow in Porous Medium

Hazim Aneed Migtaa[1,2] and Liqaa Zeki Hummady[1]
[1]*Department of Mathematics, College of Science, University of Baghdad, 10071 Baghdad, Iraq*
[2]*General Directorate of Education in Muthanna, Ministry of Education, 66001 Muthanna, Iraq*
hazem.enaid2203p@sc.uobaghdad.edu.iq, liqaa.hummady@sc.uobaghdad.edu.iq

Keywords: Peristaltic Flow, Rotation, Magnetic Felid, Stress, Electric Field.

Abstract: The peristaltic motion of a two-dimensional Williamson fluid has been analyzed within an inclined, asymmetric channel saturated with a porous medium and subjected to rotation. The system was further influenced by an externally imposed electric field and an obliquely oriented magnetic field. A presumption of a long wavelength and a low Reynolds number were used to make the analytical investigation of the nonlinear governing equations easier. Using the perturbation method, formulas for the axial velocity, pressure gradient, and stream function were methodically derived through symbolic computation using Mathematica software. A detailed investigation was then conducted into the effects of changes in physical parameters, including the flexibility of the porous matrix, rotation rate, magnetic field inclination, and the Williamson parameter, on flow properties including pressure variations, velocity distribution, and trapping phenomena. The results, supported by a detailed graphical interpretation, offer valuable insights into electro-magnetohydrodynamic (EMHD) peristaltic flow and have theoretical implications for physiological and industrial fluid systems.

1 INTRODUCTION

A physiological process known as peristalsis is defined by a series of waves of contraction and relaxation that move along the walls of a flexible conduit. This mechanism creates a variation in cross-sectional area along its length by causing periodic, involuntary constrictions and expansions in the duct through which the fluid travels. The fluid is propelled forward by the pressure gradient created by this dynamic change. The study of peristaltic transport has drawn a lot of attention in recent decades because of its important applications in biomedical engineering. Modeling and analyzing this mechanism have been the focus of much research in order to develop a variety of medical and engineering devices, such as dialysis units and blood pumping systems.

Additionally, peristaltic behavior is present in many physiological processes in the human body, including the passage of urine along the ureter, the pulsatile movement of blood in arterial vessels, and the propulsion of food through the esophagus. [1]. Because of its distinct characteristics, Williamson fluid stands out among these fluids and is the focus of numerous studies [2]. This fluid's non-Newtonian behaviours, which combines viscous and elastic viscosity [3], calls for a thorough comprehension of how it interacts with outside variables [4]. The purpose of this study is to investigate how rotation affects Williamson fluid in a porous, electrically conductive medium that experiences peristaltic motion [5], [6].

Because of its importance in numerous industrial and environmental applications, the study of electrokinetic phenomena in porous media has attracted a lot of attention. The study of electroosmotic flow in porous materials under the effects of electric and rotational fields in particular has become an important field of study. Optimizing processes ranging from drug delivery systems to water purification and oil recovery requires an understanding of how charged fluids, like electrolytes, behave in porous structures [7]-[9]. Both engineering and business can benefit from the study of MHD flow and heat transfer of a non-Newtonian fluid across a stretching sheet. For instance, a polymer sheet may occasionally be stretched during die extrusion. The final product's properties are greatly influenced by the rate of cooling. It is possible to control the cooling rate and achieve the desired properties by drawing a similar sheet in a viscoelastic electrically conducting fluid while it is exposed to a magnetic field, based on prior applications. Refs: Authors. [10]-[12] investigated MHD effects on

distinct flow problems and heat transportation along the different geometries. The pertinent investigations in Refs. [13]-[15] were carried out using a variety of mechanisms.

Physical effects of magentohdyrodynamics along with fluids characteristics over different flow geometries are discussed in Refs. [16]-[18]. In this study, we will analyse how Williamson fluid interacts with rotation in the presence of an electric field, a porous medium and an inclined magnetic field, and peristaltic. In this study, mathematical and theoretical models are employed to analyze the influence of the aforementioned factors on flow behaviours, velocity distribution, and pressure variation [2]. These effects are studied in detail using the governing equations obtained from electrohydrodynamic principles and non-Newtonian fluid theory [19]. A deeper comprehension of these phenomena and important insights into related engineering, physical, and biomedical applications are the goals of the anticipated results.

2 PROBLEM MATHEMATICAL DESCRIPTION

Consider the two-dimensional flow of the Williamson fluid in an uneven channel with width (d) through a porous medium. Triangular wave trains traveling along the channel walls at a constant speed are the source of flow [20]. The geometry of the wall structure defines the wall surface at the upper wall, which is explained as follows [20]:

$$\overline{h_1}(\overline{X},\overline{t}) = 1 + a\{\frac{8}{\pi^3}\sum_{m=1}^{\infty}\frac{(-1)^{m+1}}{(2m-1)^2}sin[(2\pi(2m-1)\overline{X})]\}$$ Lower wall, (1)

$$\overline{h_2}(\overline{X},\overline{t}) = -d - b\{\frac{8}{\pi^3}\sum_{m=1}^{\infty}\frac{(-1)^{m+1}}{(2m-1)^2}sin[(2\pi(2m-1)\overline{X}+\mathcal{E})]\}$$ Upper wall. (2)

Where (d) denotes the width of the channel, (X) indicates the direction of the wave, (t) indicates the time, and (a) and (b) represent the amplitudes of the wave. The lower and Upper walls are denoted by $\overline{h_1}(\overline{X},\overline{t})$, $\overline{h_2}(\overline{X},\overline{t})$ An asymmetric inclined channel with out-of-phase waves is represented by ($\mathcal{E}=0$) and in-phase waves by ($\mathcal{E}=\pi$). The phase difference ($\mathcal{E}$) changes in the interval ($0 \le \mathcal{E} \le \pi$). As illustrated in Figure 1, a rectangular coordinate system is adopted, where the waves are in phase. The X-axis is aligned with the direction of wave propagation, while the Y-axis is oriented perpendicular to $\bar{X}$, where $\bar{t}$ is the time.

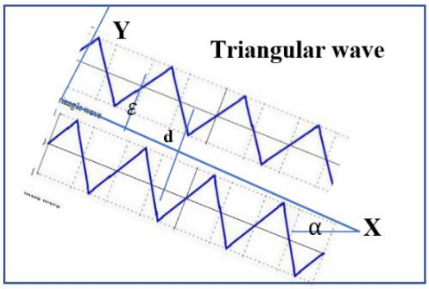

Figure 1: A physical sketch of the problem.

3 BASIC EQUATION

The expression for the Cauchy stress tensor $\bar{\tau}$corresponding to a fluid governed by the Williamson model is presented below [2]:

$$\bar{S} = -\bar{P}I + \bar{\tau}, \quad (3)$$

$$\bar{\tau} = \mu_\infty + (\mu_0 - \mu_\infty)\,[1 + (\Gamma\bar{\dot{\gamma}})^2]^{-1}\,\bar{\dot{\gamma}}. \quad (4)$$

In this context, $\bar{S}$denotes the extra stress tensor, Irepresents the identity tensor, and the gradient vector is given by $\nabla = (\partial\bar{X}, \partial\bar{Y}, 0)$. The parameters $\mu_\infty$and $\mu_0$correspond to the viscosities at infinite and zero shear rates, respectively. The shear rate $\dot{\gamma}$is then defined as follows.

$$\dot{\gamma} = \sqrt{\frac{1}{2}\text{tras}\,(\,A_{11}\,)^{\,2}}, \quad (5)$$

$$\bar{\tau} = -\mu_0\,[[1 + (\Gamma\bar{\dot{\gamma}})^2]^{-1}]\;\bar{\dot{\gamma}}, \quad (6)$$

$$A_{11} = \text{grad}\overline{V} + (\text{grad}\overline{V})^T, \quad (7)$$

$$\bar{\tau}_{\bar{x}\bar{x}} = 2\mu_0\bar{u}_{\bar{x}}(1 - (\Gamma\bar{\dot{\gamma}}^2), \quad (8)$$

$$\tau_{\bar{x}\bar{y}} = \mu_0\big(\bar{v}_{\bar{x}} + \bar{u}_{\bar{y}}\big)\big(1 - (\Gamma\overline{\dot{\gamma}})^2\big), \quad (9)$$

$$\bar{\tau}_{\bar{y}y} = 2\mu_0\bar{v}_{\bar{y}}\big(1 - (\Gamma\overline{\dot{\gamma}})^2\big). \quad (10)$$

4 THE GOVERNING EQUATION

Three pair nonlinear partial differentials of continuity and momentum, expressed in an affixed frame ($\overline{X}$, $\overline{Y}$), control the flow With the laboratory serving as a point of reference, the following equations govern flow: The equation for continuity.

$$\frac{\partial\overline{U}}{\partial\overline{X}} + \frac{\partial\overline{V}}{\partial\overline{Y}} = 0. \quad (11)$$

In X-axis:

$$\rho\left(\frac{\partial}{\partial \bar{t}}+\bar{U}\frac{\partial}{\partial \bar{x}}+\bar{V}\frac{\partial}{\partial \bar{y}}\right)\bar{U}-\rho\Omega\left(\Omega\bar{u}+2\frac{\partial\,\bar{V}}{\partial \bar{t}}\right)=-\frac{\partial \bar{p}}{\partial \bar{x}}+\frac{\partial}{\partial \bar{x}}\bar{\tau}_{\bar{x}\bar{x}}+\frac{\partial}{\partial \bar{y}}\tau_{\bar{x}\bar{y}}+\bar{p}_c E_x-\frac{\mu_0}{\bar{k}}\bar{U}+\rho g\,\mathrm{Sin}\alpha-\sigma\beta_0^2\cos\beta(U\cos\beta-V\sin\beta). \quad (12)$$

In Y-axis:

$$P\left(\frac{\partial}{\partial \bar{t}}+\bar{U}\frac{\partial}{\partial \bar{x}}+\bar{V}\frac{\partial}{\partial \bar{y}}\right)\bar{V}-\rho\Omega\left(\Omega\bar{v}-2\frac{\partial\,\bar{U}}{\partial \bar{t}}\right)=-\frac{\partial \bar{p}}{\partial \bar{x}}+\frac{\partial}{\partial \bar{x}}\tau_{\bar{x}\bar{y}}+\frac{\partial}{\partial \bar{y}}\tau_{y\bar{y}}+\bar{p}_c E_x-\frac{\mu_0}{\bar{k}}\bar{V}-\rho g Cos\alpha-\sigma\beta_0^2\sin\beta(U\cos\beta-V\sin\beta) \quad (13)$$

The famous poisson equation:

$$p_c=-\in\nabla^2\bar{\emptyset}, \quad (14)$$

$\bar{\emptyset}$ =electric potential,

$$\emptyset(y)=\frac{\sinh(y+h)k}{\sinh(2hk)}. \quad (15)$$

Here, the symbols represent the following physical quantities: ρ denotes the fluid density; $\bar{u}$ and $\bar{v}$ are the axial and transverse velocities, respectively; $\bar{y}$ is the transverse coordinate; $\bar{p}$ indicates the pressure; μ is the dynamic viscosity; $\bar{k}$ represents the permeability parameter; ϵE_x is the constant electric field; Ωdenotes the rotational parameter; and β_0^2 corresponds to the magnetic field strength. In the laboratory coordinate system $(\bar{x},\bar{y})$, the flow field is characterized as unsteady due to the continuous variation of the velocity and pressure with time. However, when the analysis is performed in a reference frame moving with the propagating wave at a constant speed c, denoted by the coordinates $(\bar{X},\bar{Y})$, the flow becomes steady relative to this moving frame.

This transformation simplifies the mathematical formulation of the problem by eliminating the explicit time dependence, allowing the governing equations to be expressed in terms of spatial variables alone. The corresponding relations between the two coordinate systems are defined as follows.

$$\bar{X}=\bar{x}-c\bar{t},\quad \bar{Y}=\bar{y},\quad \bar{U}(\bar{X},\bar{Y})=\bar{u}(\bar{x},\bar{y})-c,\quad \bar{V}(\bar{X},\bar{Y})=\bar{v}(\bar{x},\bar{y}),\ \bar{T}(\bar{X},\bar{Y})=\bar{T}(\bar{x},\bar{y},\bar{t}),\ \bar{P}(\bar{X},\bar{Y})=\bar{P}(\bar{x},\bar{y}) \quad (16)$$

5 DIMENSIONLESS PARAMETER

$$x=\frac{1}{\lambda}\bar{x},\ y=\frac{1}{d}\bar{y},u=\frac{1}{c}\bar{u},\ v=\frac{1}{\delta c}\bar{v},\ t=\frac{c}{\lambda}\bar{t},\ \delta=\frac{d}{\lambda},\ Re=\frac{\rho c d}{\mu},\ Da=\frac{\bar{k}}{d^2},\ \tau_{xx}=\frac{\lambda}{\mu c}\tau_{\bar{x}\bar{x}},$$

$$\tau_{xy}=\frac{d}{\mu c}\tau_{\bar{x}\bar{y}},\ \tau_{yy}=\frac{d}{\mu c}\tau_{\bar{y}\bar{y}},\ h_1=\frac{1}{d}\overline{h_1},Uhs=\frac{-E_x\in\varepsilon}{\mu_0 c},\ h_2=\frac{1}{d}\overline{h_2},\ We=\frac{\Gamma c}{d},\ Ha=d\sqrt{\sigma/\mu}\beta 0,\ Fr=c/gd. \quad (17)$$

Here, $\bar{u}$ and $\bar{v}$ denote the velocity components, while $\bar{p}$ represents the pressure within the wave frame of reference.

Where (δ) is the wave number, (Re) is the Reynold number (Uhs) Helmholtz-Smoluchowski velocity, (Da) Darcy number (Ha) Hartman number, (Fr) Froud number, Now that (16) and (17) has been substituted into (1), (2), and (8)–(13), the resulting equation has been normalized using the non-dimensional variables shown below:

The equation (11) becomes:

$$\frac{\partial u}{\partial x}+\frac{\partial v}{\partial y}=0, \quad (18)$$

The equation (12) becomes:

$$Re\delta\left(\frac{\partial u}{\partial t}+u\frac{\partial u}{\partial x}+v\frac{\partial u}{\partial y}\right)-\frac{d^2\Omega^2}{\mu}u-\frac{d^2 c}{\mu}\delta\frac{\partial v}{\partial t}=-\frac{\partial p}{\partial x}+\delta\frac{\partial s_{xx}}{\partial x}+\frac{\partial s_{xy}}{\partial y}+Uhs(\delta^2\frac{\partial^2\emptyset}{\partial x^2}-\frac{\partial^2\emptyset}{\partial y^2})-\frac{1}{Da}u+\frac{Re}{Fr}sin(\alpha)-Ha^2\cos\beta\,(u\cos\beta-\delta v\sin\beta \quad (19)$$

The equation (13) becomes:

$$Re\,\delta^3(\frac{\partial v}{\partial t}+u\frac{\partial v}{\partial x}+v\frac{\partial v}{\partial y})-\frac{\rho d^2}{\mu}\delta^2\Omega^2 v-\frac{2\Omega\delta^2 Re}{\lambda}\left(\frac{\partial u}{\partial t}\right)=-\frac{\partial p}{\partial y}+\delta^2\frac{\partial}{\partial x}\tau_{xy}+\delta\frac{\partial}{\partial y}\tau_{yy}+Uhs\left(\delta^2\frac{\partial^2\emptyset}{\partial x^2}+\delta\frac{\partial^2\emptyset}{\partial y^2}\right)-v\delta^2\left(\frac{1}{D_a}\right)+\delta\frac{Re}{Fr}cos(\alpha)-Ha^2\delta\sin\beta\,(u\cos\beta-\delta v\sin\beta \quad (20)$$

The equation (8) becomes:

$$\tau_{xx}=2\delta\frac{\partial u}{\partial x}\left[1-we^2\dot{Y}^2\right]. \quad (21)$$

The equation (9) becomes:

$$\tau_{xy}=\left(\delta^2\frac{\partial v}{\partial x}+\frac{\partial u}{\partial y}\right)\left[1-we^2\dot{Y}^2\right]. \quad (22)$$

The equation (10) becomes:

$$\tau_{yy}=2\delta\frac{\partial v}{\partial y}\left[1-we^2\dot{Y}^2\right]. \quad (23)$$

"The stream function ψ is related to the velocity components through the following expressions:

$$u=\frac{\partial\psi}{\partial y},v=-\frac{\partial\psi}{\partial x}. \quad (24)$$

Substituted (24) in (18), (19), (20), (21), (22), (23) respectively,

$$\frac{\partial^2\psi}{\partial x\partial y}-\frac{\partial^2\psi}{\partial x\partial y}=0, \quad (25)$$

$$Re\,\delta(\frac{\partial^2\psi}{\partial t\partial y}+\frac{\partial^3\psi}{\partial x\partial y^2}-\frac{\partial^3\psi}{\partial x\partial y^2})-\frac{\rho d^2}{\mu}\Omega^2\frac{\partial\psi}{\partial y}-\frac{2\Omega\delta Re}{\lambda}(\frac{\partial^2\psi}{\partial t\partial x})=-\frac{\partial p}{\partial x}+\delta^2\frac{\partial}{\partial x}\tau_{xx}+\frac{\partial}{\partial y}\tau_{xy}+Uhs\left(\delta^2\frac{\partial^2\emptyset}{\partial x^2}+\frac{\partial^2\emptyset}{\partial y^2}\right)-\frac{\partial\psi}{\partial y}\left(\frac{1}{D_a}\right)-Ha^2\cos\beta(\partial\Psi/\partial y\cos\beta+\delta\,\partial\Psi/\partial x\sin\beta)+\frac{Re}{Fr}sin(\alpha), \quad (26)$$

$$\mathrm{Re}\,\delta^3\left(-\frac{\partial^2\psi}{\partial t\,\partial x}+\frac{\partial^3\psi}{\partial x^2\,\partial y}-\frac{\partial^3\psi}{\partial x^2\,\partial y}\right)+\frac{\rho d^2}{\mu}\delta^2\Omega^2\frac{\partial\psi}{\partial x}-\frac{2\Omega\delta^2\mathrm{Re}}{\lambda}\left(\frac{\partial^2\psi}{\partial t\,\partial y}\right)=-\frac{\partial p}{\partial y}+\delta^2\frac{\partial}{\partial x}\tau_{xy}+\delta\frac{\partial}{\partial y}\tau_{yy}+\mathrm{Uhs}\left(\delta^2\frac{\partial^2\emptyset}{\partial x^2}+\frac{\partial^2\emptyset}{\partial y^2}\right)-\frac{\partial\psi}{\partial x}\delta^2\left(\frac{1}{D_a}\right)+\mathrm{Ha}^2\sin\beta(\delta\,\partial\Psi/\partial y\cos\beta+\delta\,\partial\Psi/\partial x\sin\beta)+\delta\frac{Re}{Fr}cos(\alpha),\quad(27)$$

$$\tau_{xx}=(2\delta)\frac{\partial^2\psi}{\partial x\,\partial y}\left[1-we^2\left(4\delta^2\left(\frac{\partial^2\psi}{\partial x\,\partial y}\right)+\left(\frac{\partial^2\psi}{\partial y^2}+\delta^2\frac{\partial^2\psi}{\partial x^2}\right)\right)(2\frac{\partial^2\psi}{\partial x\,\partial y})\right],\quad(28)$$

$$\tau_{xy}=\left(-\delta^2\frac{\partial^2\psi}{\partial x^2}+\frac{\partial^2\psi}{\partial y^2}\right)\left[1-we^2\left(4\delta^2\left(\frac{\partial^2\psi}{\partial x\,\partial y}\right)+\left(\frac{\partial^2\psi}{\partial y^2}+\delta^2\frac{\partial^2\psi}{\partial x^2}\right)\right)(\frac{\partial^2\psi}{\partial y^2})\right],\quad(29)$$

$$\tau_{yy}=-\delta\frac{\partial^2\psi}{\partial x\,\partial y}\left[1-we^2\left(4\delta^2\left(\frac{\partial^2\psi}{\partial x\,\partial y}\right)+\left(\frac{\partial^2\psi}{\partial y^2}+\delta^2\frac{\partial^2\psi}{\partial x^2}\right)\right)(2\frac{\partial^2\psi}{\partial x\,\partial y})\right].\quad(30)$$

The non-dimensional boundary conditions within the wave frame are specified as follows" [20]:

$$\psi=\frac{F}{2},\qquad\frac{\partial\psi}{\partial y}=-1\qquad\text{at y=h1,}\quad(31)$$

$$\psi=\frac{-F}{2},\qquad\frac{\partial\psi}{\partial y}=-1\qquad\text{at y=h2.}\quad(32)$$

6 SOLUTION OF THE PROBLEM

Obtaining an exact analytical solution for all the arbitrary parameters involved in the governing equations is generally not feasible due to the inherent complexity and nonlinear nature of the problem. The perturbation technique is used to get around this problem and get a decent approximation of the system's behaviour. This analytical technique allows for successive approximations by expanding the governing equations in terms of a small parameter. This method makes it easier to systematically examine the flow characteristics and sheds light on how different physical parameters affect the system's overall behaviour.

$$\psi=\psi_0+\mathrm{We}^2\,\psi_2+\mathrm{O}(\mathrm{We}^4),\mathrm{P}=P_0+we^2P_2+\mathrm{O}(we^4)$$
$$\mathrm{F}=\mathrm{F}_0+\mathrm{We}^2\mathrm{F}_2+\mathrm{O}(\mathrm{We}^4),\quad(33)$$

By changing the expressions given in Equation (33) into the Equations (25)–(30), along with the boundary conditions specified in Equations (31) and (32), and considering the assumption that $\delta \ll 1$, the higher-order terms containing powers of $\delta$are regarded as negligibly small and therefore omitted from the analysis. Consequently, a reduced and simplified system of equations is obtained by collecting and equating the coefficients corresponding to identical powers of the wave number parameter We. This procedure allows the derivation of successive approximations for the dependent variables, facilitating a clearer understanding of the dominant flow behavior at each order of approximation. From Eq. (26) and Eq. (29) we get:

$$-\frac{\rho d^2}{\mu}\Omega^2\frac{\partial\psi}{\partial y}=-\frac{\partial p}{\partial x}+\frac{\partial}{\partial y}\tau_{xy}+\mathrm{Uhs}\left(\frac{\partial^2\emptyset}{\partial y^2}\right)-\frac{\partial\psi}{\partial y}\left(\frac{1}{D_a}\right)-\mathrm{Ha}^2\cos\beta(\frac{\partial\psi}{\partial y}\cos\beta)+\frac{Re}{Fr}sin(\alpha),\quad(34)$$

$$\tau_{xy}=\left(\frac{\partial^2\psi}{\partial y^2}\right)\left[1-we^2\left(\left(\frac{\partial^2\psi}{\partial y^2}\right)\right)(\frac{\partial^2\psi}{\partial y^2})\right].\quad(35)$$

From differential of y for Eq. (34)

$$-\frac{\rho d^2}{\mu}\Omega^2\frac{\partial}{\partial y}\left(\frac{\partial\psi}{\partial y}\right)=\frac{\partial}{\partial y}\tau_{xyy}+\mathrm{Uhs}\frac{\partial}{\partial y}\left(\frac{\partial^2\emptyset}{\partial y^2}\right)-\frac{\partial}{\partial y}\left(\frac{\partial\psi}{\partial y}\left(\frac{1}{D_a}\right)\right)-\mathrm{Ha}^2\cos\beta\frac{\partial}{\partial y}\left(\frac{\partial\psi}{\partial y}\cos\beta\right).\quad(36)$$

From Eq (27) we get:

$$-\frac{\partial p}{\partial y}=0.\quad(37)$$

6.1 Zero Order System

By neglecting the terms of order (We) in the zeroth - order formulation, the governing system reduces to the following form:

$$\psi_{0yyyy}+\mathrm{Uhs}\,\emptyset_{yyy}-\frac{1}{\mathrm{Da}}\psi_{0yy}+\frac{\rho d^2}{\mu}\Omega^2\,\psi_{0yy}-\mathrm{Ha}^2(\cos\beta)^2\psi_{0yy}=0.\quad(38)$$

Such that

$$\psi_0=\frac{F_0}{2},\qquad\frac{\partial\psi_0}{\partial y}=-1\text{ at}\qquad y=\text{h.1,}\quad(39)$$

and

$$\psi_0=-\frac{F_0}{2},\qquad\frac{\partial\psi_0}{\partial y}=-1\text{ at}\qquad y=\text{h.2.}\quad(40)$$

6.2 Sconed Order System

$$\psi_{2yyyy}-\frac{\partial^2}{\partial y^2}\left(\psi_{0yy}\right)^3+\mathrm{Uhs}\,\emptyset_{yyy}-\frac{1}{\mathrm{Da}}\psi_{2yy}+\frac{\rho d^2}{\mu}\Omega^2\,\psi_{2yy}-\mathrm{Ha}^2(\cos\beta)^2\psi_{2yy}=0,\quad(41)$$

$$\psi_2=-\frac{F_1}{2},\frac{\partial\psi_2}{\partial y}=-1\text{ at y=h.1,}\quad(42)$$

$$\psi_2=-\frac{F_1}{2},\frac{\partial\psi_2}{\partial y}=-1\text{ at y= h.2.}\quad(43)$$

By solving the corresponding zeroth- and second-order systems, the final expression for the stream function can be derived as follows.

$$\psi = \psi_0 + We^2\,\psi_2, \tag{44}$$

the axial velocity:

$$u = \psi_y, \tag{45}$$

the pressure gradient:

$$\frac{\partial p}{\partial x} = \frac{\rho d^2}{\mu}\Omega^2\frac{\partial \psi}{\partial y} + \frac{\partial}{\partial y}\tau_{xy} + Uhs\left(\frac{\partial^2 \emptyset}{\partial y^2}\right) - \frac{\partial \psi}{\partial y}\left(\frac{1}{D_a}\right) - Ha^2\cos\beta\left(\frac{\partial \psi}{\partial y}\cos\beta\right) + \frac{Re}{Fr}sin(\alpha). \tag{46}$$

7 FINDINGS AND DISCUSSION

In order to study the effect of various physical parameters such as the effect of, Darcy number (Da), Reynolds number (Re), Rotation (Ω), the Weissenberg number (We), (Uhs), Helmholtz-smoluchowski velocity, (Ha) Hartman number, (Fr) Froud number, (β)inclined magnetic, (α)inclined channel and ($\mathcal{E}$) phase different, the plotted axial velocity (u), and pressure gradient ($\frac{\partial p}{\partial x}$) in Figures 2 - 9. are illustrated using the software "MATHEMATICA".

Equation of momentum has been solved using the perturbation technique, and the corresponding results are presented and analyzed graphically.

7.1 Axial Velocity

Figures 2, 5, 6 and 9 demonstrate that the axial velocity exhibits a progressive enhancement with the increase in the Darcy number (Da), the inclination angle parameter (β), the Hartmann number (Ha), and the dimensionless distance (d). This behaviour indicates that the permeability of the porous medium, magnetic field intensity, and geometrical expansion collectively facilitate the momentum transfer along the axial direction. The velocity continues to rise until it attains a maximum value, beyond which it gradually declines and approaches its steady-state level, suggesting the presence of a dynamic equilibrium between viscous resistance and electromagnetic forces.

On the other hand, Figures 3, 4, 7 and 8 show that as the Weissenberg number (We), rotation parameter (Ω), porosity parameter (ϵ), and upper wall velocity (Uhs) increase, the axial velocity decreases. Until a critical turning point is reached, the velocity decrease continues, and then the flow magnitude mildly recovers.

The combined effect of viscoelastic relaxation and rotational effects is indicated by this non-monotonic trend, in which elastic stresses first predominate and cause velocity suppression, followed by a re-acceleration phase as inertial effects become more significant. Interestingly, the variation with respect to Weis is nonlinear, exhibiting an inflection point that represents the change from dominant regimes that are elastic to those that are viscous.

7.2 Pressure Gradient Distribution $\left(\frac{dp}{dx}\right)$

As the Darcy number (Da), rotation parameter (Ω), Hartmann number (Ha), and upper wall velocity (Uhs) increase, the pressure gradient $\left(\frac{dp}{dx}\right)$ rises nonlinearly, as shown in Figures 10-13. The intricate interplay between the inertial, magnetic, and viscous forces controlling the flow dynamics is reflected in this nonlinear enhancement. The permeability of the porous medium improves with an increase in Darcy number, permitting more fluid penetration and producing a steeper pressure gradient along the axial direction. This behavior is further influenced by the rotational parameter (Ω), which introduces centrifugal and Coriolis effects that intensify the axial pressure variation and redistribute the momentum field.

Furthermore, the Lorentz force, which opposes fluid motion and necessitates a greater driving pressure to maintain the same flow rate, amplifies the pressure gradient through the Hartmann number (Ha). In a similar vein, raising the upper wall velocity (Uhs) increases the shear stresses close to the boundary, strengthening the pressure gradient because of the increased momentum exchange between the fluid and the wall. Since magnetic, rotational, and hydrodynamic effects are strongly coupled, the observed nonlinear trend of $\left(\frac{dp}{dx}\right)$ emphasizes the dominance of magnetohydrodynamic (MHD) interactions on the general pressure distribution.

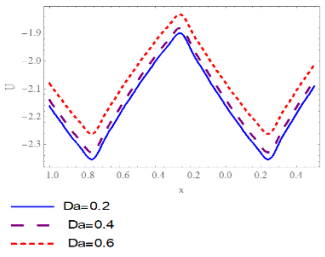

Figure 2: Velocity distribution.

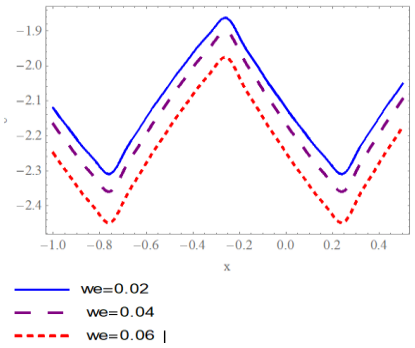

Figure 3: Velocity distribution.

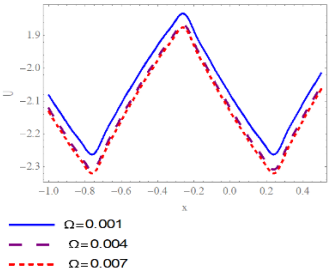

Figure 4: Velocity distribution.

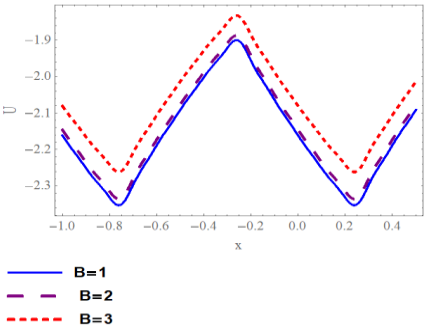

Figure 5: Velocity distribution.

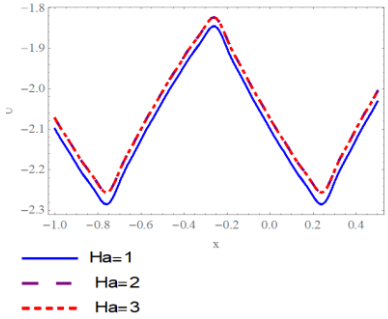

Figure 6: Velocity distribution.

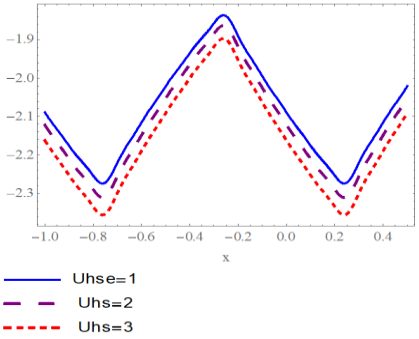

Figure 7: Velocity distribution.

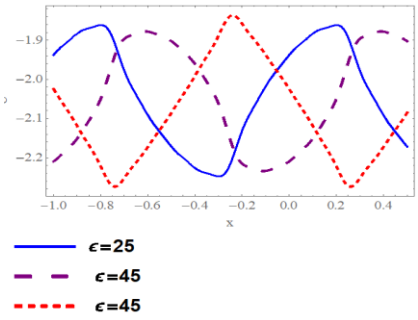

Figure 8: Velocity distribution.

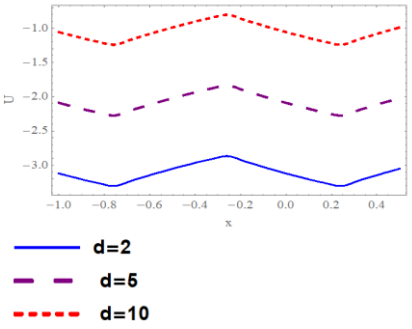

Figure 9: Velocity distribution.

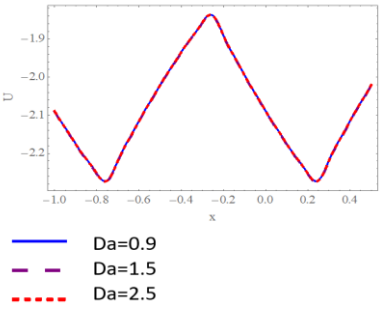

Figure 10: Presser distribution.

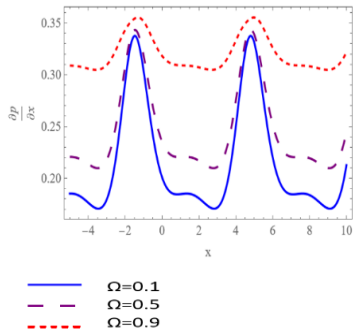

Figure 11: Presser distribution.

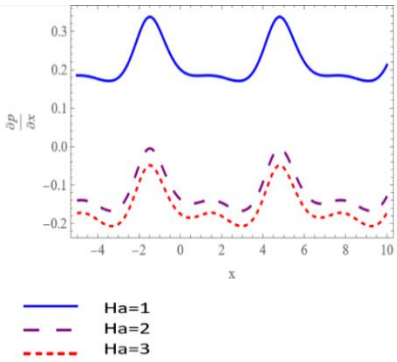

Figure 12: Presser distribution.

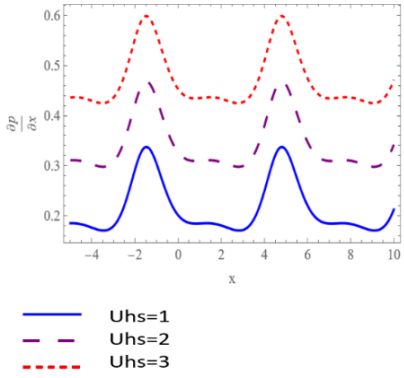

Figure 13: Presser distribution.

8 CONCLUSIONS

The current research provides a holistic analysis and assessment of the momentum transfer processes responsible for magnetohydrodynamic (MHD) flow in a porous medium driven by the simultaneous effects of permeability parameters, rotation effects, magnetic interactions, and viscoelastic constitutive parameters. It is observed from the findings that the axial velocity simultaneously increases with the increase in Darcy number, angle of inclination, Hartmann number, and scaled distance; this implies that the higher the permeability and the interactions between the permeable material and the magnetic field, the more efficient the momentum transfer process. However, larger Weissenberg number, rotation parameter, porosity parameter, and velocity on the upper wall lead to a simultaneous reduction in velocity.

Additionally, the nonlinear increase with respect to the Darcy number, rotation parameter, Hartmann number, and speed on the upper wall highlights the coupling between the processes. It is this coupling that is vital for pressure and energy considerations for this particular flow. The observations also confirm that pressure and velocity are highly coupled with magnetohydrodynamic processes, especially when viscoelastic effects coexist with permeability and magnetism.

In general, this research depicts that the combination of effects such as magnetic field forces, porosity parameters, rotational motions, and viscoelasticity is responsible for the behavior of flows within the porous media. These aspects can be used for further research on the behavior of flows under the influence of MHD and can be employed for optimal design and development approaches for various heat transfer and filtration processes.

ACKNOWLEDGMENTS

The Department of Mathematics, College of Science, University of Baghdad, Baghdad, Iraq, is deeply appreciated by the authors for its invaluable assistance and resources, which greatly aided in the completion of this study.

REFERENCES

[1] H. Abdulhussein and A. M. Abdulhadi, “Impact of couple stress and rotation on peristaltic transport of a Powell–Eyring fluid in an inclined asymmetric channel with Hall and Joule heating,” Journal of Basic Sciences, vol. 8, no. 13, 2022.

[2] Zehra, M. M. Yousaf, and S. Nadeem, “Numerical solutions of Williamson fluid with pressure-dependent viscosity,” Results in Physics, vol. 5, pp. 20-25, 2015.

[3] A. M. Abdulhadi and T. S. Ahmed, “Effect of magnetic field on peristaltic flow of Williamson fluid through a porous medium in an inclined tapered asymmetric channel,” Mathematics & Theory and Modeling, vol. 7, pp. 549-565, 2017.

[4] Z. A. Jaafar, L. Z. Hummady, and M. H. Thawi, "Effects of rotation and inclined magnetic field on Walters' B fluid in a porous medium using the perturbation method," Iraqi Journal of Science, pp. 818-827, 2024.

[5] R. G. Ibraheem and L. Z. Hummady, "Powell–Eyring fluid peristaltic transfer in an asymmetric channel and porous medium under rotation and inclined magnetic field," Iraqi Journal of Science, pp. 6431-6444, 2023.

[6] A. Aziz, W. Jamshed, T. Aziz, H. M. S. Bahaidarah, and K. Ur Rehman, "Entropy analysis of Powell–Eyring hybrid nanofluid including the effect of linear thermal radiation and viscous dissipation," Journal of Thermal Analysis and Calorimetry, vol. 143, no. 2, pp. 1331-1343, 2021, , [Online]. Available: https://doi.org/10.1007/s10973-020-10210-2.

[7] N. T. Eldabe, K. A. Kamel, S. F. Ramadan, and R. A. Saad, "Peristaltic motion of Eyring–Powell nanofluid with couple stresses, heat, and mass transfer through porous media under a magnetic field inside an asymmetric vertical channel," Journal of Advanced Research in Fluid Mechanics and Thermal Sciences, vol. 68, no. 2, pp. 58-71, 2020.

[8] M. S. Ramadhan and K. K. Jassim, "Impact of inclined magnetic field and rotation on peristaltic flow of viscoelastic fluid with variable viscosity," vol. 28, no. 3-A, pp. 729-740, 2025.

[9] H. N. Mohaisen, "Influence of rotation and inclined magnetic field with mixed convective heat and mass transfer in an inclined symmetric channel on peristaltic flow with slip conditions," Iraqi Journal of Science, pp. 6460-6476, 2023.

[10] E. Infeld, "Review of Magnetic Reconnection: MHD Theory and Applications, by E. R. Priest and T. G. Forbes, Cambridge Univ. Press, 2000," Journal of Plasma Physics, vol. 66, no. 5, pp. 363-367, 2001.

[11] W. K. Sadiq and D. G. Al-Khafajy, "Influence of heat transfer on MHD oscillatory flow for Williamson fluid with variable viscosity through a porous medium," International Journal of Fluid Mechanics & Thermal Sciences, vol. 4, pp. 11-17, 2018.

[12] K. Kavita, K. R. Prasad, and B. A. Kumari, "Influence of heat transfer on MHD oscillatory flow of Jeffrey fluid in a channel," Advances in Applied Science Research, vol. 3, no. 4, pp. 2312-2325, 2012.

[13] M. M. Hamza, B. Y. Isah, and H. Usman, "Unsteady heat transfer to MHD oscillatory flow through a porous medium under slip condition," International Journal of Computer Applications, vol. 33, no. 4, pp. 12-17, 2011.

[14] J. A. Falade, J. C. Ukaegbu, A. C. Egere, and S. O. Adesanya, "MHD oscillatory flow through a porous channel saturated with porous medium," Alexandria Engineering Journal, vol. 56, pp. 147-152, 2017.

[15] D. G. Al-Khafajy, "Radiation and mass transfer effects on MHD oscillatory flow for Jeffrey fluid with variable viscosity through a porous channel in the presence of a chemical reaction," Scientific International (Lahore), vol. 31, no. 2, pp. 223-228, 2019.

[16] D. G. Al-Khafajy, "Effects of heat transfer on MHD oscillatory flow of Jeffrey fluid with variable viscosity through porous medium," Advances in Applied Science Research, vol. 7, no. 3, pp. 179-186, 2016.

[17] S. O. Adesanya and O. D. Makinde, "MHD oscillatory slip flow and heat transfer in a channel filled with porous media," Romanian Journal of Physics, vol. 76, pp. 197-204, 2014.

[18] B. P. Garg, K. D. Singh, and A. K. Bansal, "Hall current effect on viscoelastic (Walter's liquid model-B) MHD oscillatory convective channel flow through a porous medium with heat radiation," Kragujevac Journal of Science, vol. 36, pp. 19-32, 2014.

[19] A. M. Jasim, "Study of the impact of unsteady squeezing magnetohydrodynamics copper-water with injection-suction on nanofluid flow between two parallel plates in porous medium," Iraqi Journal of Science, pp. 3909-3924, 2022.

[20] D. G. S. Al-Khafajy, "Influence of varying temperature and concentration on magnetohydrodynamics peristaltic transport for Jeffrey fluid with a nanoparticles phenomenon through a rectangular porous duct," Baghdad Science Journal, vol. 18, no. 2, p. 7, 2021.